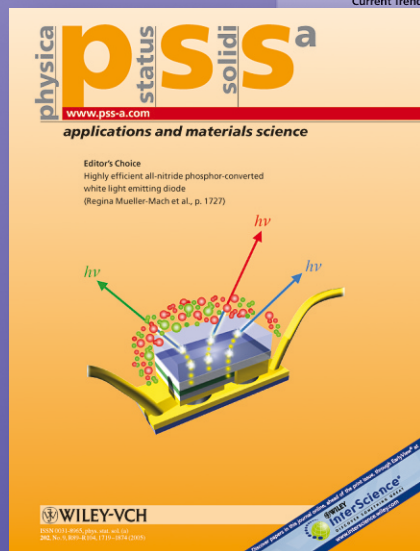


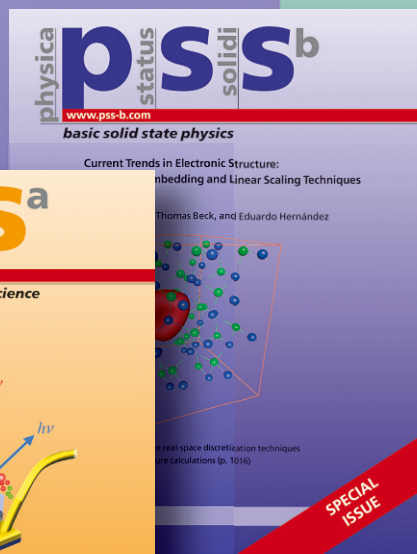
physica p status solidi S S

www.interscience.wiley.com

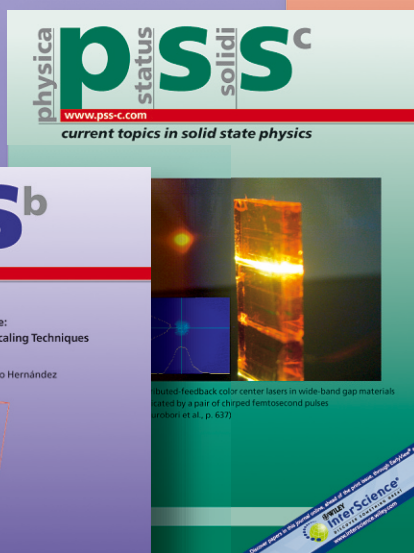
reprints



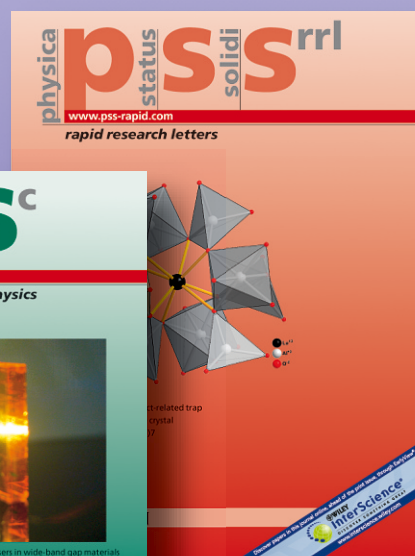
www.pss-a.com



www.pss-b.com



www.pss-c.com



www.pss-rrl.com

Pore growth on n-type InP investigated by in-situ FFT impedance spectroscopy

Malte Leisner*, Jürgen Carstensen, Ala Cojocar, and Helmut Föll

Institute for Materials Science, Christian-Albrechts-University of Kiel, Kaiserstraße 2, 24143 Kiel, Germany

Received 7 March 2008, revised 24 October 2008, accepted 17 November 2008

Published online 5 February 2009

PACS 81.05.Ea, 81.05.Rm, 82.45.Qr, 84.37.+q

* Corresponding author: e-mail ml@tf.uni-kiel.de, Phone: +49 431 880 6180, Fax: +49 431 880 6178

In this work in-situ FFT impedance spectroscopy is applied to analyze the growth of current-line oriented pores in (100) oriented n-type InP. A fitting model based on standard electrical equivalent elements is developed, which yields very consistent and good results during the course of long-time etching experiments. An analysis based on the time and parameter dependence of the fitting parameters, as well as a measurement of the pore depth as a function of etching time, allows to identify the physico-chemical reactions and processes related to the different parts of the impedance. The interface (reac-

tion) at the pore tips, a mass transfer phenomenon inside the pores, as well as a third process located outside the pores are observed. The characteristic behavior of these processes under variations of the electrolyte concentration or the applied external potential yields a deep insight into the total pore formation process: The potential drop over the interface at the pore tips could be identified to be independent of the HCl concentration or applied external potential. The mass transfer process is directly responsible for the total current flowing, and thus for the growth rate of the pores.

© 2009 WILEY-VCH Verlag GmbH & Co. KGaA, Weinheim

1 Introduction Pore growth on n-type InP has been observed in a variety of electrolytes. The “standard” electrolyte in this case has been HCl, in the last years some groups have successfully demonstrated that pores can be formed with electrolytes like KOH [1] or liquid ammonia [2]. For HCl electrolytes the resulting pores can be basically grouped into two classes according to their geometry and growth direction. The so-called crystallographically oriented pores (crystos) grow along $\langle 111 \rangle_B$ directions, their tips and walls have a defined crystallographic orientation as well, for a full treatise of this topic see e.g. [3]. The history of these pores dates back to the 1960s, when tunnels were observed during the electrochemical thinning of GaAs [4, 5] and GaP [6]. In InP the first crystos have been observed by Takizawa et al. [7] and later been reproduced by some groups [8, 9]. The other pores are current-line oriented pores (curros); these pores grow perpendicular to the equipotential lines, and thus usually perpendicular to the sample surface. Since the first experimental results of Kikuno et al. emerged [10], these pores have been reproduced and studied by several [8, 9, 11–15].

Even though the aforementioned amount of work has been carried out in this field, little knowledge about the

pore growth mechanisms of cristo and curro pores exists. To get a deeper insight into the mechanisms constituting pore growth on n-type InP, in-situ FFT impedance spectroscopy (FFT IS) measurements have been performed during the pore etching experiments. The term FFT IS refers to “Fast Fourier Transform” impedance spectroscopy [16, 17], an advanced mode of the classical impedance spectroscopy, in which all frequencies are applied in one signal, thus reducing the measurement time for an individual measurement drastically, and enabling stable (FFT) impedance spectroscopy measurements during pore etching experiments. This measurement technique has already been successfully applied to macropore growth on n-Si and related experiments [18–21]. Besides the mentioned deficit of knowledge about the pore growth on n-type InP, there exist no in-situ impedance spectroscopy measurements as well. Even ex-situ measurements are very rare, for the n-type InP/HCl system only the work of Hens and Gomes [22] exists so far, which has been carried out under slightly different conditions, e.g. with front side illumination and only at small anodic potentials.

In this work we will focus on the current-line oriented pores and will present first results on the impedance of this

system. The time-dependant impedance parameters will be analyzed in the framework of a model for the growth of curro pores on n-type InP.

2 Experimental setup All experiments have been performed on wafer pieces cut from (100) oriented n-type InP with a doping concentration of $N_D = 10^{17} \text{ cm}^{-3}$. HCl aq. with differing concentrations was used as electrolyte. The experiments have been performed in an electrochemical double cell described in full detail in [23] without further illumination and at a temperature $T = 20 \text{ }^\circ\text{C}$. The InP was etched at constant anodic potentials. To achieve a homogeneous nucleation, experiments have been started by a voltage pulse of 15 V for 1 s.

The FFT impedance spectroscopy measurements have been performed by a system produced by ET&TE GmbH. Measurements were taken at 1.5 s intervals. The signal contained 27 frequencies in the range between 50 Hz and 20 kHz.

3 Experimental results

3.1 Pores An example for the type and quality of the obtained pores is given in Fig. 1. These pores have been grown under optimized conditions of $U = 11 \text{ V}$, and 6 wt% HCl.

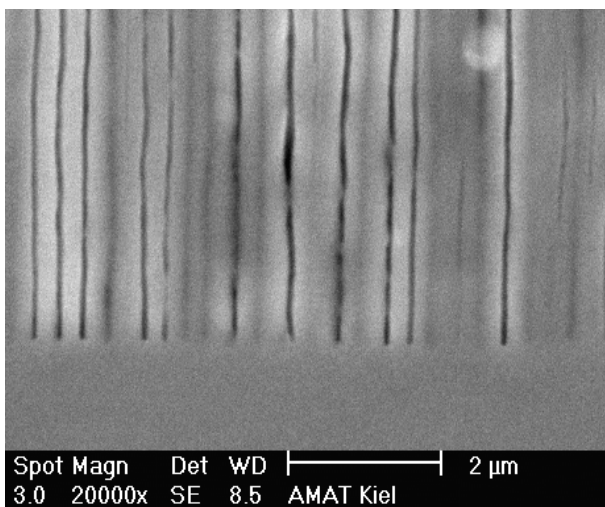


Figure 1 Curro pores in n-InP. SEM micrograph of current-line oriented pores etched under optimized conditions: $U = 11 \text{ V}$, and 6 wt% HCl.

Typical current-line oriented pores have been etched, with a quite high homogeneity, thus enabling reasonable FFT impedance measurements. Since these measurements are the main topic of these work, the following part of the manuscript will be exclusively devoted to the impedance results. For a deeper treatise of aspects like morphology and pore structure, as well as parameter dependance, the

interested reader is referred to [8]. The manuscript will basically discuss the results of one series of experiments performed under optimized conditions (11 V, 6 wt% HCl) for different etching times. The results of other parameter variations will be partly included, whenever they are able to deliver more non-redundant information in respect to the main series.

3.2 Impedance data The impedance measurements during the growth of current-line oriented pores yielded very consistent results. Figure 2 illustrates the measurement for an experiment with a constant potential of 11 V and an electrolyte concentration of 6 wt% HCl at 22 min of the total etching time of 70 min. Shown are (a) the Nyquist Plot and (b) the corresponding Bode Plots. The measured data is represented by dots, whereas the lines represent the fitting function, which is matching the data very well. The function used to fit the data is given by

$$Z(\omega) = R_s + \frac{R_1}{1 + i\omega\tau_1} - \frac{R_2}{1 + (1+i)\sqrt{\omega\tau_2}} + \frac{R_3}{1 + i\omega\tau_3}, \quad (1)$$

with $\tau_2 = R_2^2 / 2 \sigma^2$, $\tau_1 = R_1 C_1$, and $\tau_3 = R_3 C_3$.

This model corresponds to an equivalent circuit consisting of a serial resistance R_s in series with two time constants τ_1 and τ_3 , in series with a Warburg impedance, characterized by the parameters τ_2 and σ , in parallel to the resistance R_2 . R_1 , R_2 , and R_3 describe the respective transfer resistances. Different other fit models with 7 or less fit parameters have been tried as well, but yielded only unsatisfactory results, thus lending credibility to the applied fitting model.

Since the impedance measurements have been performed in-situ during the pore growth every 1.5 seconds, the aforementioned fitting parameters can safely be plotted as a function of time. The resulting curves are shown in Fig. 3 for the same 70 min pore etching experiment.

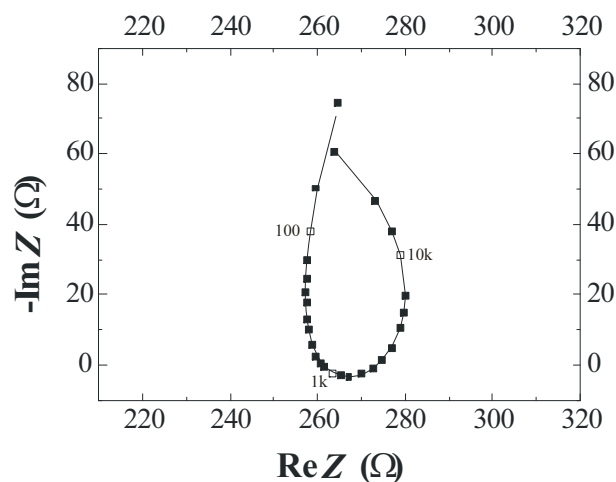
The time dependance of some parameters will be explicitly named here, since they play an important role in the discussion part. The resistance R_2 shows a time dependance according to

$$R_2 = 29.0 \Omega \left(\frac{t}{\text{min}} \right)^{0.4}. \quad (2)$$

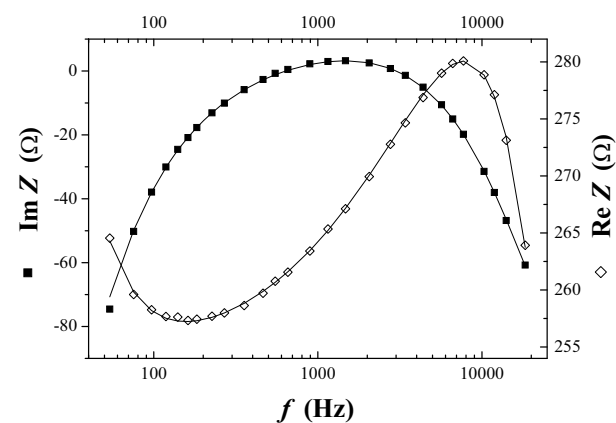
The time constant τ_2 shows a linear time dependance:

$$\tau_2 = 1.32 \mu\text{s} + 0.13 \frac{\mu\text{s}}{\text{min}} \cdot t. \quad (3)$$

Figure 4 shows the results of a set of 12 experiments conducted at a constant potential of 11 V with an electro-



(a)



(b)

Figure 2 Typical (a) Nyquist Plot and (b) Bode Plots for an impedance measurement with $U = 11$ V, 6 wt% HCl at 22 min of the pore growth experiment. The symbols represent the measured data, the lines indicate the fitting function Eq. (1). The measurement frequencies in Hz are indicated in (a).

lyte concentration of 6 wt%. The etching time was changed between the experiments and the resulting pore depth l_{pore} at the end of the experiment has been measured.

The resulting data is plotted in form of squares and shows a characteristic time behavior that can be well expressed by

$$d_{\text{pore}} = 35.7 \mu\text{m} \left(\frac{t}{\text{min}} \right)^{0.60} \quad (4)$$

The derivation of this function with respect to the time yields v_{tips} , the etching speed at the pore tips:

$$v_{\text{tips}} = 21.4 \frac{\mu\text{m}}{\text{min}} \left(\frac{t}{\text{min}} \right)^{-0.40} \quad (5)$$

This curve is also shown in Fig. 4 on a second scale.

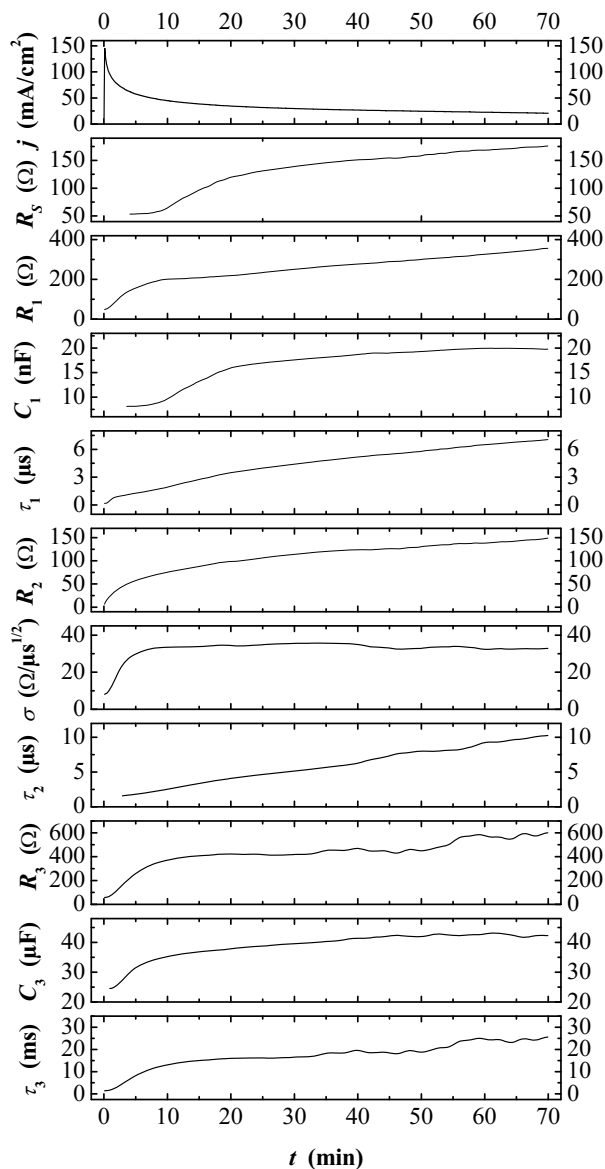


Figure 3 Time dependence of the current density and the impedance parameters. The time dependence of the current density and the fitting parameters contained in the model described in Eq. (1) is plotted. The impedance curves have been smoothed by averaging to remove the measurement inherited noise.

4 Discussion The discussion will be structured according to the equivalent circuit of the fitting model (cf. Eq. (1) and the corresponding part of the manuscript text), i.e. any logical group of elements belonging to one chemical reaction or process will be discussed separately.

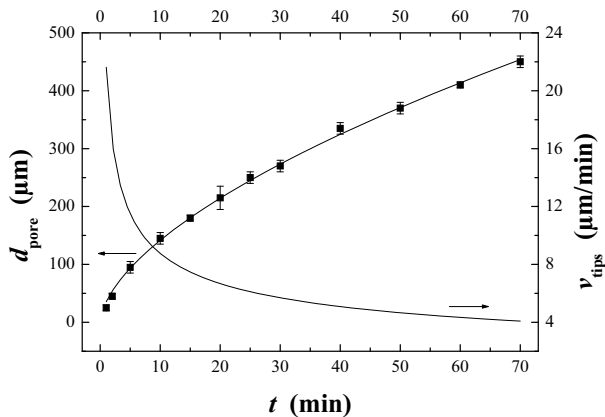


Figure 4 Pore depth d_{pore} and growth rate v_{tips} as function of the etching time. The dots represent individual pore depth measurements, the functionality of $d_{\text{pore}}(t)$ can be well described by Eq. (4). The growth rate can be obtained through deriving, its functionality is given in Eq. (5).

4.1 $R_1 / C_1 / \tau_1$ Figure 5 illustrates the product of the resistance R_1 and the current I as a function of etching time. For times $t < 10$ min the curve changes significantly, afterwards it stays rather constant at an equivalent potential of roughly 1.8 V. SEM measurements (not shown here) clearly show that in the first 5-10 min of any experiment the pores are in a nucleation phase, i.e. pore growth is not homogenous and equiaxially directed. For etching times $t > 10$ min very homogenous pore growth is observed. The mentioned times coincide very well with the characteristics of the curve in Fig. 1. For stable pore growth $I R_1 = \text{constant}$ holds, i.e. the process / reaction has to run under a constant potential drop for the formation of good quality pores.

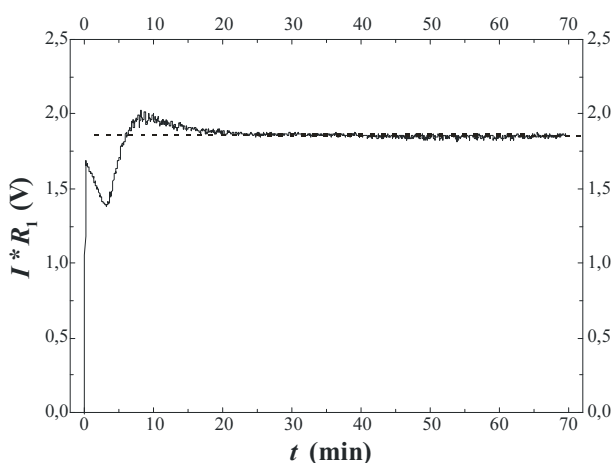


Figure 5 Time dependance of the product current I times the resistance R_1 . The curve shows a significant change in the first 10 minutes. Afterwards it is constant at an equivalent potential of roughly 1.8 V.

4.2 $R_2 / \tau_2 / \sigma_2$ The general nature of the fitting parameters R_2 , τ_2 , and σ_2 is already obvious from the partial equivalent circuit corresponding to these parameters, it contains a Warburg impedance parallel to a resistance. It is well known, that diffusion in the electrolyte can play an important role during pore growth in n-type InP, e.g. as a diffusion limitation, which is necessary for stable pore growth [8]. Thus, it is highly probable that the process underlying these parameters is a diffusion process. A closer look at the parameter dependencies will yield more information about the nature of this process: The time dependance of the resistance R_2 has already been presented in Eq. (2). The time dependance of the growth rate v_{tips} has been given in Eq. (5) and shows a proportionality of $1/v_{\text{tips}} \propto R_2$. This means that the resistance R_2 belonging to the diffusion process is governing the growth rate of the pores. From the fitting model it is evident that R_2 is directly linked to the Warburg impedance, and thus the diffusion phenomenon. Since the diffusion process is linked to the transfer of ions in the electrolyte through the length of the pores, the resistance R_2 has to be spatially linked to this process, i.e. it will also represent a process/reaction in through the length of the pores.

The transport through the pores, either by diffusion of ions in the pores or by the ohmic process represented by R_2 , thus is the rate limiting process during the growth of current-line oriented pores in n-InP.

4.3 $R_3 / C_3 / \tau_3$ The time dependance of the fitting parameters R_3 , C_3 , and τ_3 for the third process / reaction share one common characteristic. They show significant changes during the first 10 min of the experiment. Afterwards they only show slight or no changes at all. As already discussed in Section 4.1, the first 10 min belong to the nucleation of pores, afterwards stable pore growth occurs. This means that whatever is described by the third process, it can only distinguish between two states: pores exist and pores do not exist. If the pores have nucleated, further pore growth does not influence the process anymore, or in other words: the process is not dependant on the pore depth (and thus on e.g. ohmic losses).

4.4 Variation of the HCl concentration As mentioned in Section 2, experiments with different HCl concentrations have been performed. Due to the restricted space of the manuscript, from the large variety of interesting results just the most prominent will be presented here.

One interesting finding is that the product of the current I and the resistance R_1 after the nucleation phase is the same constant equivalent potential of 1.8 V, as it was shown for 6 wt% HCl in Fig. 5, for all electrolyte concentrations in the range of (3-7) wt%.

Another interesting behavior is observed for the time constant τ_2 . In Fig. 3 it was already shown to have a linear dependance on the etching time. The same linear slope is found in experiments with the aforementioned differing

HCl concentrations. The only difference is the starting point for $t = 0$ min, i.e. the curves show the same slope and have an offset only, which depends on the HCl concentration.

5 Conclusion The growth of current-line oriented pores has been analyzed with in-situ FFT impedance spectroscopy. The resulting impedance could be fitted very well and consistently with the fitting model presented in Eq. (1) under the variation of various etching parameters (etching time, HCl concentration, applied potential, temperature). Three semicircles are present in the Nyquist-Plot (cf. Fig. 2) representation of the impedance, which can be linked to three reactions / processes.

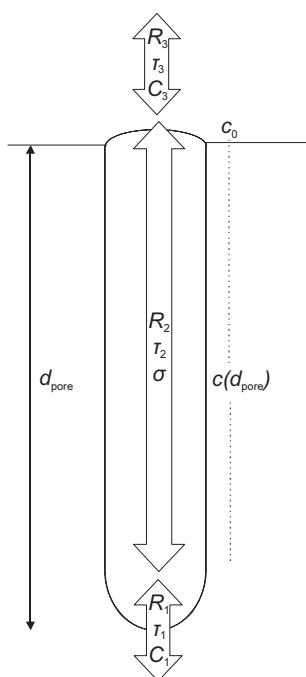


Figure 6 Schematic representation of the interpretation of the impedance data. The parameters with index 1 describe the charge transfer and capacitance of the semiconductor electrolyte interface at the pore tips. The parameters with index 2 belong to a mass transfer in the pores. Parameters with index 3 could belong to a chemical reaction/process outside the pores.

These reactions are interpreted according to the schematic illustration of pore growth in Fig. 6. Reaction/process 1 describes the interface reaction/capacitance. The constant potential drop (Fig. 5) is characteristic for stable and good pore growth. Reaction / process 2 describes the transfer of ions through the electrolyte. The diffusion related parameters show a linear time dependance (τ_2), resp. a constant behavior in the stable pore growth region (σ). The ohmic part (R_2) is proportional to the growth rate v_{tips} . The reaction / process 2 is the rate determining reaction / process for the growth of current-line oriented pores in n-type InP. Reaction/process 3 is not dependant on the pore depth. Thus it could be a reaction outside of the pores as indicated in Fig. 6. Another possible explanation could be, that it is a partial reaction of the total reaction at the pore tips. Further work will be necessary to clarify this question.

In the same vein, further experiments have to be carried out to get more information about the individual processes. Especially, similar impedance spectroscopy measurements will be carried out during the growth of crystallographically oriented pores to obtain a wider understanding of the pore formation in InP.

References

- [1] C. O'Dwyer, D. N. Buckley, D. Sutton, and S. B. Newcomb, *J. Electrochem. Soc.* **153**(12), G1039 (2006).
- [2] A. M. Gonçalves, L. Santinacci, A. Eb, I. Gerard, C. Mathieu, and A. Etcheberry, *Electrochem. Solid-State Lett.* **10**(4), D35 (2007).
- [3] E. Spiecker, M. Rudel, W. Jäger, M. Leisner, and H. Föll, *Phys. Status Solidi A* **202**(15), 2950 (2005).
- [4] J. P. Krumme and M. E. Straumanis, *Trans. Met. Soc. AIME* **239**, 395 (1967).
- [5] M. M. Faktor, D. G. Fiddymant, and M. R. Taylor, *J. Electrochem. Soc.* **122**(11), 1566 (1975).
- [6] B. D. Chase and D. B. Holt, *J. Electrochem. Soc.* **119**(3), 314 (1972).
- [7] T. Takizawa, S. Arai, and M. Nakahara, *Jpn. J. Appl. Phys.* **33**(2, 5A), L643 (1994).
- [8] H. Föll, S. Langa, J. Carstensen, S. Lölkes, M. Christophersen, and I. M. Tiginyanu, *Adv. Mater.* **15**(3), 183 (2003).
- [9] H. Tsuchiya, M. Hueppe, T. Djenizian, and P. Schmuki, *Surface Science* **547**(3), 268 (2003).
- [10] E. Kikuno, M. Amiotti, T. Takizawa, and S. Arai, *Jpn. J. Appl. Phys.* **34**(1, 1), 177 (1995).
- [11] A. Hamamatsu, C. Kaneshiro, H. Fujikura, and H. Hasegawa, *J. Electroanal. Chem.* **473**, 223 (1999).
- [12] H. Hasegawa and T. Sato, *Electrochim. Acta* **50**, 3015 (2005).
- [13] A. Liu, *Nanotechnology* **12**, L1 (2001).
- [14] P. Schmuki, L. Santinacci, T. Djenizian, and D. J. Lockwood, *Phys. Status Solidi A* **182**(1), 51 (2000).
- [15] H. Fujikura, A. Liu, A. Hamamatsu, T. Sato, and H. Hasegawa, *Jpn. J. Appl. Phys.* **39**(7B), 4616 (2000).
- [16] G. S. Popkurov and R. N. Schindler, *Rev. Sci. Instrum.* **63**, 5366 (1992).
- [17] G. S. Popkurov, *Electrochimica Acta* **41**(7/8), 1023 (1996).
- [18] J. Carstensen, E. Foca, S. Keipert, H. Föll, M. Leisner, and A. Cojocar, *Phys. Status Solidi A* **205**(11), 2485 (2008).
- [19] E. Foca, J. Carstensen, G. Popkurov, and H. Föll, *ECS Trans.* **6**(2), 345 (2007).
- [20] E. Foca, J. Carstensen, G. Popkurov, and H. Föll, *Phys. Status Solidi A* **204**(5), 1378 (2007).
- [21] S. Keipert, J. Carstensen, and H. Föll, *ECS Trans.* **6**(2), 387 (2007).
- [22] Z. Hens and W. P. Gomes, *J. Phys. Chem. B* **104**, 7725 (2000).
- [23] S. Langa, I. M. Tiginyanu, J. Carstensen, M. Christophersen, and H. Föll, *Electrochem. Solid-State Lett.* **3**(11), 514 (2000).